Available online at www.sciencedirect.com
ScienceDirect
Trans. Nonferrous Met. Soc. China 32(2022) 217−232
Transactions of Nonferrous Metals Society of China
www.tnmsc.cn

Effect of ECAP processing on distribution of second phase particles, hardness and electrical conductivity of Cu−0.81Cr−0.07Zr alloy

Filipe CALDATTO DALAN[1], Gisele Ferreira de LIMA ANDREANI[1], Dilermando Nagle TRAVESSA[1], Ilshat Albertovich FAIZOV[2], Svetlana FAIZOVA[3], Kátia Regina CARDOSO[1]

1. Institute of Science and Technology, Federal University of São Paulo, 330 Talim St., São José dos Campos, 12231-280, Brazil;
2. Institute for Metals Superplasticity Problems RAS, 39 S. Khalturin St., Ufa, 450001, Russia;
3. Ufa State Aviation Technical University, 12 K. Marx St., Ufa, 450008, Russia

Received 14 January 2021; accepted 20 August 2021

Abstract: The effect of equal-channel angular pressing (ECAP) processing at room temperature and 300 °C on the distribution of the second phase particles and its influence on hardness and electrical conductivity of the commercial Cu−0.81Cr−0.07Zr alloy were investigated. Microstructural characterization indicated that the area fraction of coarse Cr-rich particles decreased after ECAP processing. This reduction was attributed to the Cr dissolution induced by plastic deformation. The electrical conductivity of the alloy decreased by 12% after 4 ECAP passes at room temperature due to the increase of electrons scattering caused by higher Cr content in solid solution and higher density of defects in the matrix. These results were supported by the reduction of the Cu lattice parameter and by the exothermic reactions, during differential scanning calorimetry (DSC) analysis, observed only in the samples subjected to ECAP processing. Aging heat treatment after ECAP processing promoted an additional hardening effect and the complete recuperation of the electrical conductivity, caused by the re-precipitation of the partially dissolved particles. The better combination of hardness (191 HV) and electrical conductivity (83.5%(IACS)) was obtained after 4 ECAP passes at room temperature and subsequent aging at 380 °C for 1 h.

Key words: ECAP; Cu−Cr−Zr alloy; second phase particles; phase transition

1 Introduction

Cu−Cr and Cu−Cr−Zr alloys are of great interest in the electric/microelectronics industry, due to their excellent combination of mechanical strength and electrical conductivity, which are usually inverse properties. PURCEK et al [1] described a wide range of industrial applications of these alloys that comprise spot welding electrodes, power transmission cables, heat exchangers and thermonuclear reactor components. These alloys are strengthened by cold work, the precipitation of nanometric chromium particles, and Cu−Zr intermetallic phases when zirconium is present in the chemical composition [2,3]. Nevertheless, the high electrical conductivity is attributed to the low solid solubility of Cr in Cu [4].

SHANGINA et al [5] reported an increase in the mechanical strength and thermal stability of the Cu−Cr−Zr alloys, with different chemical compositions, through aging heat treatment performed after plastic deformation. This hardening effect results from the dislocation−particle interaction, described by Orowan mechanism, besides the grain boundaries pinning effect. However, the plastic deformation after aging is also an efficient processing route to improve mechanical

Corresponding author: Filipe CALDATTO DALAN, E-mail: caldatto.filipe@gmail.com
DOI: 10.1016/S1003-6326(21)65789-8

properties and can provide important information to understand the interaction between deformation structures and second phase particles.

Due to the low solid solubility of the alloying elements in copper and to the inherent limitations of conventional plastic deformation process, severe plastic deformation (SPD) methods have been considered by the scientific community as an alternative route to increase the mechanical strength of these alloys without significant reduction in the electrical conductivity [6−10]. VINOGRADOV et al [7] obtained hardness and electrical conductivity superior to commercial alloys, in a Cu−0.44Cr−0.2Zr alloy, aged after SPD processing, and an excellent correlation between structure and properties. However, to be a competitive method to produce commercial alloys, the SPD processing route should be attractive for use in industrial scale, since these methods can be complex and present limitation of geometry and size of products.

VALIEV and LANGDON [8] described that among the SPD methods, the equal-channel angular pressing (ECAP) is a promising method to be used as an additional step in the production cycle, due to the possibility of obtaining simple and constant cross-section products. However, in order to reach advanced properties, a wide range of micro-structural parameters must be controlled. ECAP processing usually results in ultra-fine grained structure (UFG) and, according to FAIZOVA et al [11], when applied in precipitation hardenable alloys it can result in changes in the morphology, size and distribution of second phase particles. These results are important to demonstrate the role of second phase particles in deformed structures [11]. However, a detailed study of the interaction between the second phase particles and deformation structures must be accomplished to optimize the process parameters in order to reach mechanical and electrical properties desirable to industrial applications.

The ECAP processing also affects the phase transformation kinetics, since the high shear forces imposed to the material during the process generate a high density of dislocations and vacancies, enhancing the atomic mobility and acting as preferential sites for particles nucleation. FAIZOV et al [12] discussed the role of morphology and chemical composition of the second phase particles in the phase transformation kinetics. Although there is the excellent agreement between results and hypothesis, the evolution of second phase particles during SPD processing and the involved mechanisms are very complex.

Several studies focused on the microstructural evolution during ECAP process and its influence on functional properties of Cu−Cr−Zr alloys. LEÓN et al [9] evaluated the effect of microstructural evolution on strength and ductility. PURCEK et al [1] investigated the effects of grain refinement on mechanical properties, correlating with the wear behavior. MISHNEV et al [13] studied the deformation microstructures and the strengthening mechanisms. However, the influence of ECAP process on the second phase particles is still poorly discussed and not completely understood in the literature. Therefore, this work aims to study the evolution of the second phase particles during ECAP processing and evaluate the effects of changes in morphology, size and distribution on the hardness and electrical conductivity of the commercial Cu−Cr−Zr alloy.

2 Experimental

2.1 Materials and methods

Commercial cold worked (drawn) and aged cylindrical bars of the Cu−Cr−Zr alloy, with nominal composition of Cu−0.81Cr−0.07Zr (wt.%), were used in this study. Billets having 10 mm in diameter and 50 mm in length were machined from the bars and subjected to ECAP processing up to 4 passes using the route B_C, in which the sample was rotated 90° in the same direction around their longitudinal axis between successive passes. The ECAP processing was performed with 20 mm/min pressing velocity, under two conditions of room temperature (RT) and 300 °C. Copper-based lubricant paste was used in order to reduce the friction between samples and die, improving the surface finishing of the samples and reducing the ECAP load. A die with circular cross-section and channel intersection angle of 120°, and with a curvature radius different of zero, was employed, as shown in Fig. 1. This construction geometry results in a true strain (ε) of 0.7 per pass, according to the equation proposed by IWAHASHI et al [14]. The friction factor was disregarded due to the use of the lubricant.

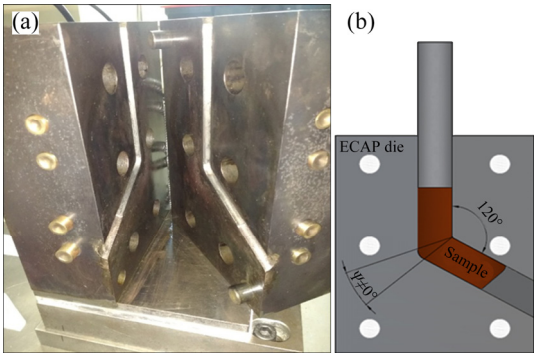

Fig. 1 Schematic illustration (a) and geometry (b) of ECAP die

2.2 Microstructure, phase, hardness, and electrical conductivity

In order to perform a complete microstructural characterization of the bars subjected to ECAP, samples were taken in both longitudinal and transversal directions. Samples with 3 mm in thickness and 10 mm in diameter were taken from the cross-section of the billets and mechanically ground in a fine sequence of grinding with SiC paper up to 2500 grit, to perform X-ray diffraction, hardness, and electrical conductivity measurements. Figure 2 schematically shows the methodology employed for the obtained samples for the characterization.

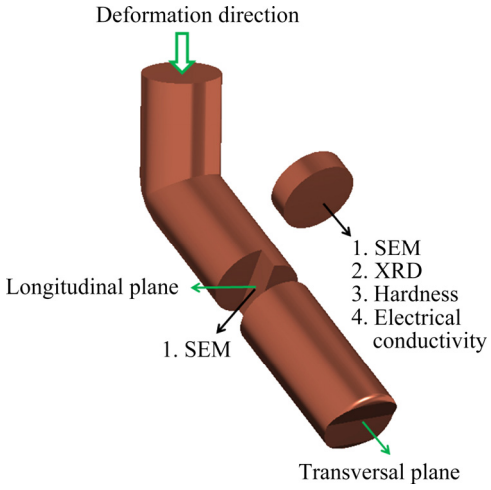

Fig. 2 Schematic illustration of sample geometry, planes, and processing direction

The microstructural characterization was carried out by scanning electron microscopy (SEM) in an FEI INSPECT S50 microscope. The grain boundaries were revealed by etching with a solution of ferric chloride (5 g $FeCl_3$ + 10 mL HCl + 100 mL H_2O) for 15 s at room temperature. The average grain size was estimated using the line intercept method, in 8 different regions of the samples, randomly chosen. Backscattered electron detector (BSD) was employed to better identify the Cr-rich precipitates. Eight different regions of the samples were randomly chosen, corresponding to 0.16 mm² of sample area analyzed. ImageJ software was employed to evaluate the evolution of morphology, distribution and average size (Ferret diameter) of the second phase particles after ECAP passes.

Mechanical properties were assessed by Vickers hardness (HV) test under a load of 98 N and a holding time of 20 s. Electrical conductivity was evaluated in a ZAPPI DC−11M eddy-current conductivity instrument, with an accuracy of ±1%. The measurements were performed at room temperature and the results were expressed as a percentage of the International Annealed Copper Standard (%(IACS)). The hardness and electrical conductivity values correspond to the average of five measurements.

Thermal analyses were performed by differential scanning calorimetry (DSC) in a Netzsch DSC 204 F1 Phoenix. The phase transition temperatures were determined under constant heating rate of 10 °C/min. The phases present were identified by X-ray diffractometry (XRD). A Rigaku Ultima IV was used with Cu K_α radiation, and the samples were analyzed on their transversal section. The lattice parameters were determined by the Rietveld refinement method using the MAUD software.

3 Results and discussion

3.1 Effect of ECAP processing on microstructure

Figure 3(a) shows the microstructure of the alloy in the as-received condition. Typical metals that crystallize in face-centered cubic (FCC) structure, annealing and deformation twins, some indicated by arrows in Detail A, are present due to standard industrial thermo-mechanical processing. Figure 3(b) shows a higher magnification image along with the elemental microanalysis X-ray spectrum (EDS) of one of the second phase particles, which are Cr-enriched, and un-dissolved during the solution treatment, as also reported by LEÓN et al [9]. As the Cr content in the alloy formulation exceeds the maximum equilibrium

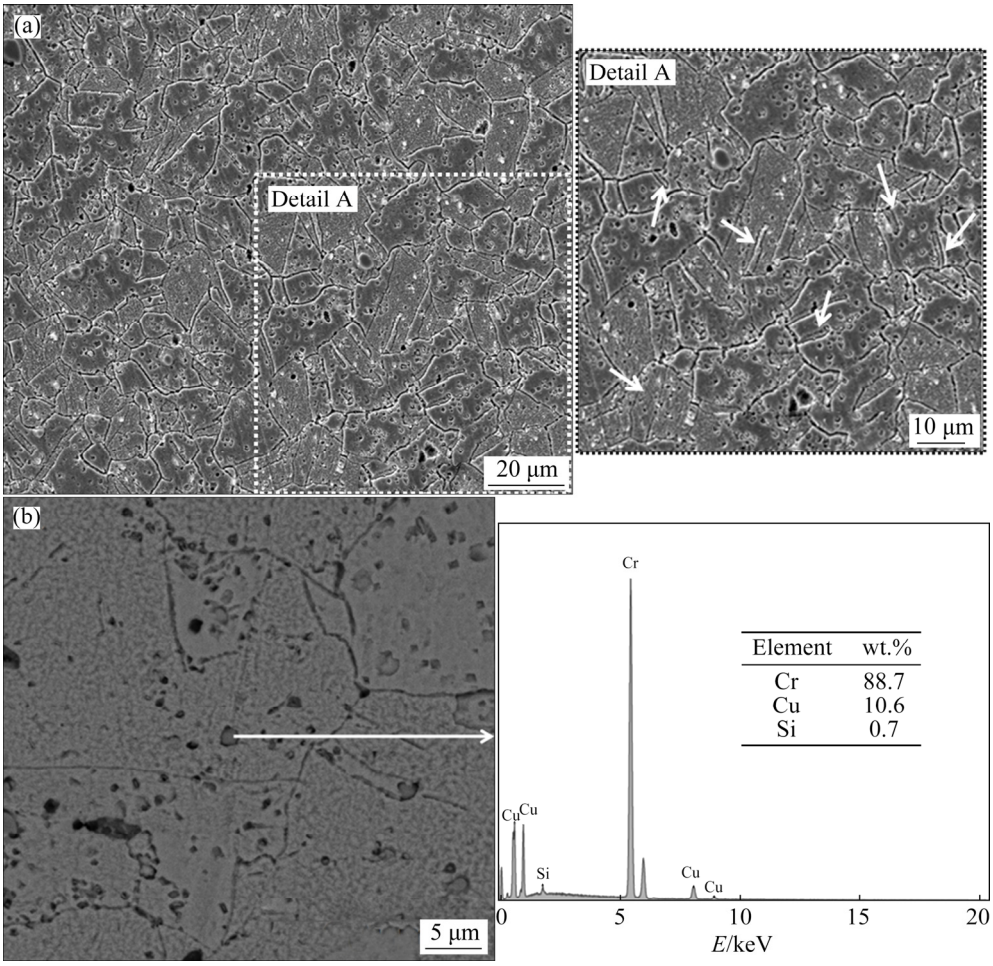

Fig. 3 Microstructural aspect of Cu−0.81Cr−0.07Zr (transverse plane) in as-received condition: (a) General aspect of microstructure with detail area expanded (Image obtained by SEM with SE detector); (b) EDS spectrum of coarse second phase particle in microstructure (Image obtained by SEM with BSE detector)

solid solubility of Cr in Cu, which is near to 0.71 wt.% at 1076 °C [4], the presence of coarse second phase particles is expected in the microstructure. These particles do not contribute to a relevant improvement on mechanical strength, since they are incoherent with the matrix and widely spaced from each other, being unlikely to interact with dislocations by the Orowan mechanism [9]. The presence of Cu and Si (impurity) refers to the contribution of the elements from the matrix.

Figure 4 shows the evolution of the microstructure after 1 (Figs. 4(a, c)) and 4 (Figs. 4(b, d)) ECAP passes at room temperature. After the first pass, the grains retain their elongated form resulting from the drawing process (see Fig. 4(a)). According to VALIEV and LANGDON [8], after the first ECAP pass, the first deformation bands, which are in regions of high density of low-angle grain boundaries, are formed. After 4 ECAP passes, the microstructure presents a high density of deformation bands and the average grain size decreases (see Fig. 4(b)). The microstructural changes during ECAP processing can be discussed in terms of the evolution of the low-angle dislocation cells formed inside the original grains, to a high-angle recrystallized structure, agreeing results reported by with MOROZOVA et al [15], during warm deformation, and SUN et al [16], during deformation at room temperature.

Similar behavior is observed after ECAP processing at 300 °C (Fig. 5). However, the grain refinement in this case is not so pronounced as in the case of room temperature processing. These results agree with MISHNEV et al [13], since the thermal energy favors recovering mechanisms, and reducing the stored energy for recrystallization.

The microstructures observed in longitudinal planes (Figs. 4(a, b) and Figs. 5(a, b)) show a tendency for the formation of elongated grains

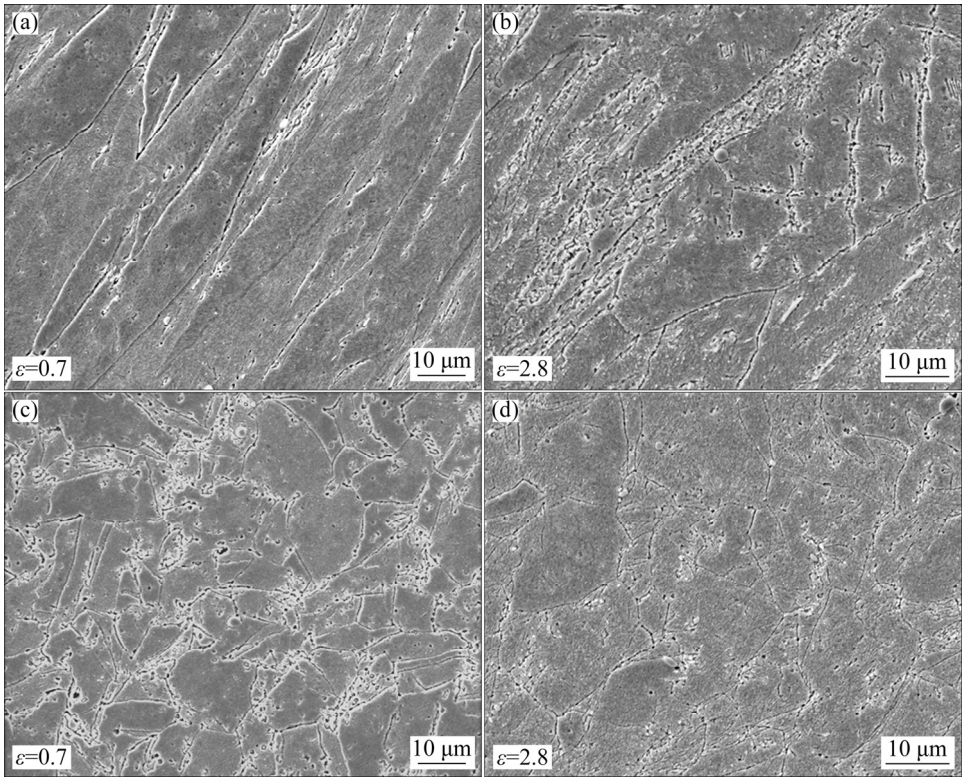

Fig. 4 Microstructures of Cu−0.81Cr−0.07Zr alloy after ECAP processing at room temperature (Images obtained by SEM with SE detector): (a) 1 ECAP pass, longitudinal plane; (b) 4 ECAP passes, longitudinal plane; (c) 1 ECAP pass, transversal plane; (d) 4 ECAP passes, transversal plane

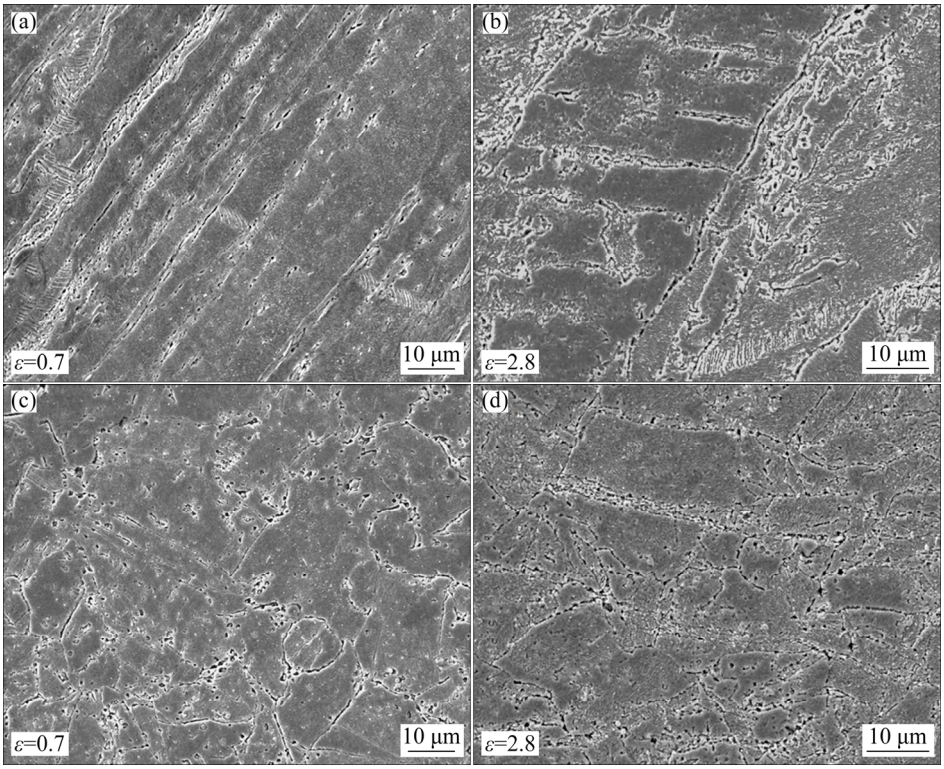

Fig. 5 Microstructures of Cu−0.81Cr−0.07Zr alloy after ECAP processing at 300 °C (Images obtained by SEM with SE detector): (a) 1 ECAP pass, longitudinal plane; (b) 4 ECAP passes, longitudinal plane; (c) 1 ECAP pass, transversal plane; (d) 4 ECAP passes, transversal plane

aligned with the ECAP direction, while fragmented grains are seen in the transversal plane (Figs. 4(c, d) and Figs. 5(c, d)). During ECAP processing by the route B_C, due to the sample rotation between each pass through the ECAP die, different slip systems are activated, which will influence the formation of microstructure. Its influence is better seen in the transversal plane, presenting refined grains.

It is important to mention the heat generated during the ECAP processing, resulting from the shearing of the crystallographic planes, with a consequent increase in the sample temperature. It has been reported that the temperature increase occurs more expressively in samples deformed at high pressing speeds [17,18]. The increase in temperature during the ECAP processing can be disregarded in this work considering the low pressing speed (20 mm/min) that was used. Another factor to be considered is the resistance of the material to pass through the shearing zone. Materials with higher values of mechanical strength tend to present a considerable increase in the sample temperature during plastic deformation [17]. The analysis of the influence of heat generated during deformation by ECAP on microstructural evolution is beyond the scope of this work, but it is worth emphasizing its importance in the formation of the microstructure.

The average grain sizes of the samples subjected to ECAP, as well as of the as-received sample, were correlated to the Vickers hardness values in Table 1. It is important to note that the average grain size measurements in the longitudinal plane were performed regarding to the width of the elongated grains. It is clearly seen that the reduction in grain size is more pronounced when the sample is processed at room temperature. On the longitudinal section, the grains width decreases, although a slight elongation has been observed in the ECAP direction as shown in Figs. 4(a, b) and Figs. 5(a, b). Estimation of the average grain size after 4 ECAP passes, in both processing conditions, was not performed by SEM images. In this case, the complexity of the microstructure, which is caused by high density of deformation bands coexisting with the pre-existing grains (grains from the as-received condition), makes the conventional SEM/line intercept method useless for this purpose.

Processing by ECAP at room temperature is the most effective for increasing hardness, as well as for grain refinement, as previously shown. This behavior can be attributed to the increase in the grain boundary area and dislocation density, according to the Hall−Petch and Taylor relations, respectively, as reported and well discussed by MOROZOVA and KAIBYSHEV [19].

Table 1 Average grain sizes with respective hardness of Cu−0.81Cr−0.07Zr alloy in as-received condition and after ECAP processing

Condition	Average grain size/μm		Hardness (HV)
	Longitudinal	Transversal	
As-received	19.8	14.9	170±5
1 ECAP pass at RT	10.7	10.8	178±3
4 ECAP passes at RT	–	–	188±4
1 ECAP pass at 300 °C	12.5	14.5	169±5
4 ECAP passes at 300 °C	–	–	176±4

3.2 Effect of ECAP processing on coarse second phase particles

The effect of ECAP processing on the morphology, average size, and distribution of coarse second phase particles in the copper matrix was also analyzed by SEM. In this case, no chemical etching was performed. Instead, images were obtained using backscattered electrons detector that allows atomic number contrast to better identify the second phase particles. In the as-received condition, these particles have morphology near to spherical with an average size of a few micrometers and are randomly dispersed in the microstructure, as can be seen in Fig. 6(a). Figure 6(b) refers to the same figure, after the conversion to a binary image by saturation of pixels intensity at different levels. It allows to easily obtain a satisfactory contrast of the bright phase (second phase particles in the upper half of the image) and their edges (lower half of the image), being essential to obtain the average Ferret diameter and the number and fraction of the particles. Table 2 shows the compilation of the data obtained from the quantitative image analysis of the samples in all processing conditions.

From Table 2, it can be observed that the area fraction of the second phase particles decreases after ECAP, mainly in the samples processed at room temperature. This is more evident in the cross-

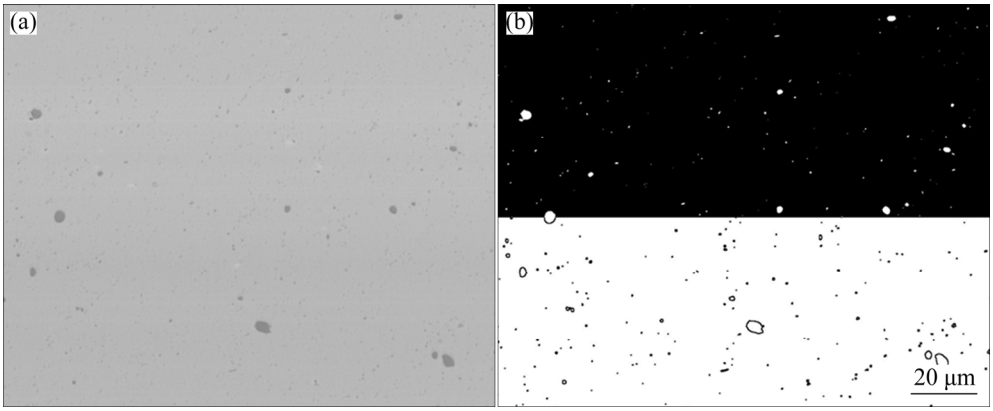

Fig. 6 Phase contrast of Cu matrix and Cr-rich second phase particles of Cu−0.81Cr−0.07Zr alloy (Typical images used for the quantitative second phase particles analysis): (a) Image obtained by SEM using BSE detector; (b) Same image after threshold (upper) and phase edges (lower) treatments

Table 2 Area fraction, average number and average Ferret diameter of coarse second phase particles of Cu−0.81Cr−0.07Zr alloy in as-received condition and after ECAP processing

Condition	Area fraction of second phase particles		Average number of second phase particles		Average Ferret diameter/μm	
	Longitudinal	Transversal	Longitudinal	Transversal	Longitudinal	Transversal
As-received	0.86	0.79	319	374	1.45	1.85
1 ECAP pass at RT	0.74	0.49	174	196	1.87	1.43
4 ECAP passes at RT	0.57	0.42	151	150	1.52	1.26
1 ECAP pass at 300 °C	0.92	0.56	318	375	1.68	1.06
4 ECAP passes at 300 °C	0.62	0.51	142	90	1.63	2.49

section of the samples, presenting the lowest values after 4 passes of ECAP. The same trend is observed for the average number of particles, which can be attributed to the interactions between these particles and structural defects, as reported by LIU et al [20]. They proposed that the non-equilibrium grain boundaries, developed during the formation of the UFG structure, presenting a high density of dislocations formed through the sliding bands, interact with the second phase particles. This interaction changes their morphology and dimensions. In Fig. 7, in addition to the dimensional changes, it can be observed that, after ECAP processing, the particles are preferentially located at the grain boundaries (single arrows), and assuming an elongated morphology aligned to the ECAP direction (double arrows). The overall result is a homogenous distribution of the second phase particles in the copper matrix, resulting from their interaction with dislocations and new grain boundaries generated by the fragmentation of the pre-existing grains.

FAIZOV et al [12] evidenced that coarse Cr particles can be dissolved during severe plastic deformation of Cu−Cr−Zr alloys. The increased diffusivity, resulting from the higher density of defects, favors the diffusion-controlled phase transformations, like particles dissolution, enhanced by the mechanical fragmentation process. In the present work, this fragmentation is not evident from the average Ferret diameter shown in Table 2. Although the fraction area of the second phase has been reduced after ECAP on both longitudinal and transversal sections, their average Ferret diameter did not change significantly, remaining mostly in the range of 0.5−1.5 μm (see Fig. 8). However, when analyzing the particle size distribution histograms in Fig. 8, interesting aspects can be observed. Comparing the particle size distribution in the as-received bar with those in samples deformed by ECAP, it is evident that the number of the submicrometric particles decreases significantly after ECAP, suggesting that they may have been fragmented, or even have dissolved. Furthermore,

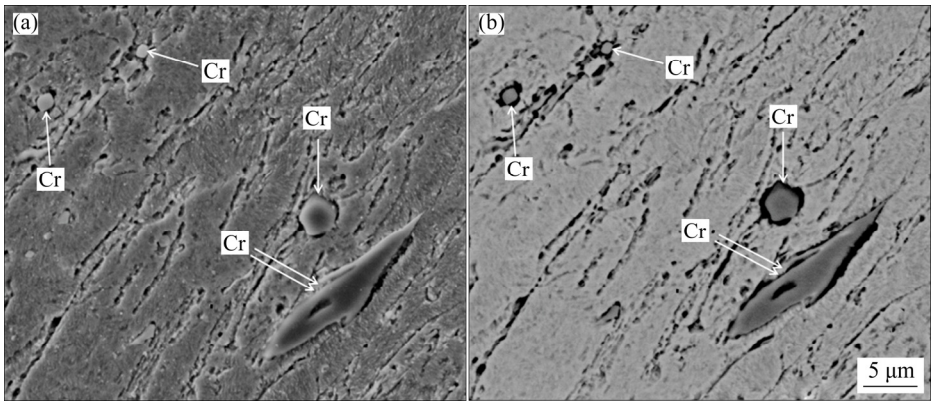

Fig. 7 Microstructures of Cu−0.81Cr−0.07Zr alloy after 4 ECAP passes at room temperature (Arrows indicate Cr particles in longitudinal plane: (a) Image obtained by SEM with SE detector; (b) Image obtained by SEM with BSE detector

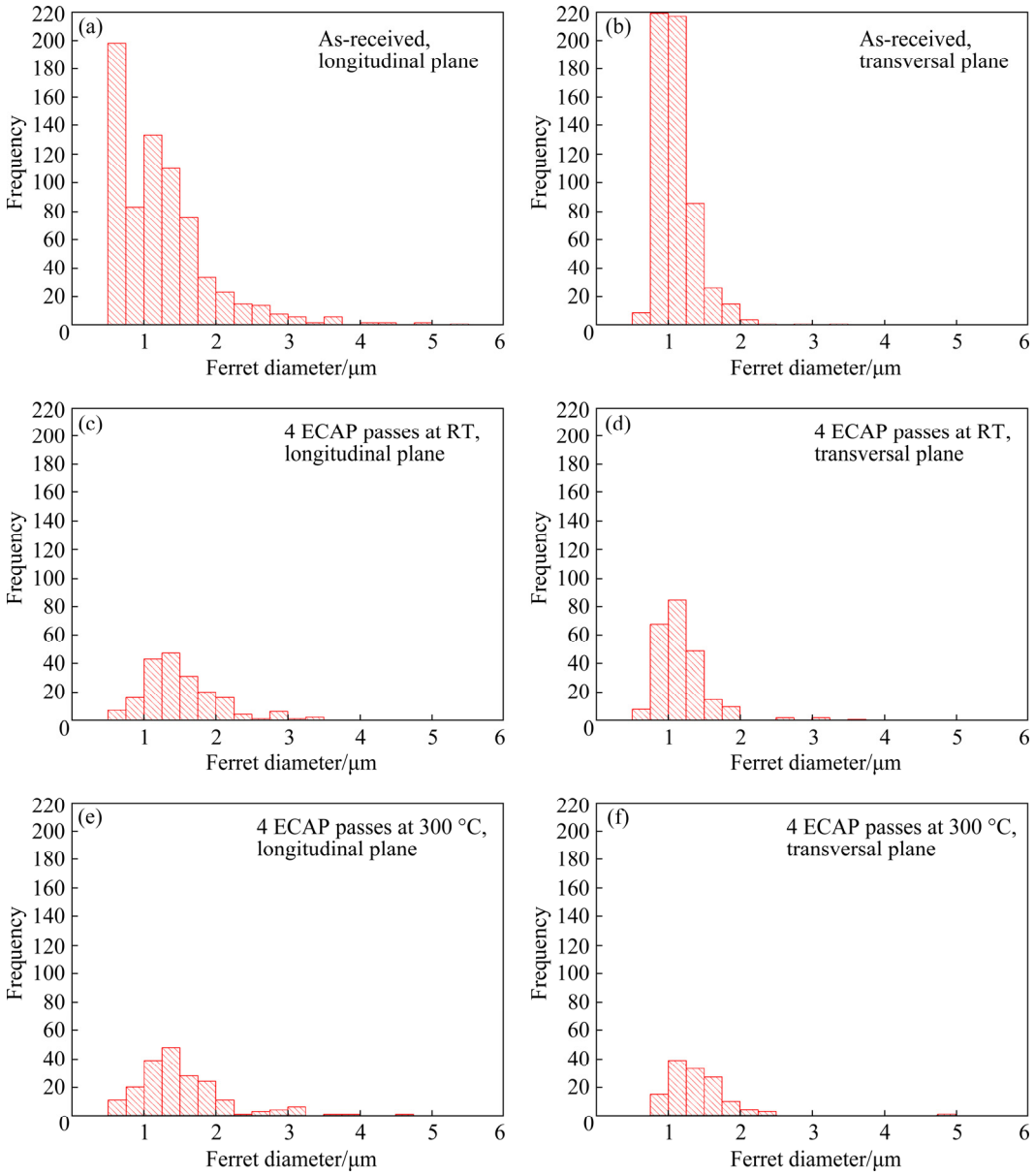

Fig. 8 Histograms of Ferret diameter of Cu−0.81Cr−0.07Zr alloy in different conditions: (a, b) As-received; (c, d) After 4 ECAP passes at room temperature; (e, f) After 4 ECAP passes at 300 °C

the number of particles of a few micrometers in size also decreases, suggesting that they are fragmented during the high deformation process. These results agree with FAIZOVA et al [21], mentioning that the SPD processing results in a significant decrease in the number of second phase particles, which is related to the deformation-induced dissolution of these particles, where the mechanical fragmentation has an important role. In addition to fragmentation and dissolution, the particle morphology also changes from spherical to irregular shape; this can be seen by comparing the particles in the as-received condition (Fig. 6) and after ECAP processing (Fig. 7). Some particles are even elongated in the processing direction, assuming the form of thin ribbons. This morphology on the transversal section after 4 ECAP passes is uncommon, as the adopted processing route (route B_C) imposes perpendicular shear pattern planes, fragmenting particles, and grains along their lengths in subsequent ECAP passes.

Nevertheless, it is important to mention that, in addition to coarse second phase particles, nanometric Cr-rich particles, generated during aging step in the standard industrial thermo-mechanical processing, are present in the micro-structure in all processing conditions. These particles are responsible for increasing the mechanical strength of the alloy by increasing the dislocations and grain boundaries pin effects [13,22,23]. LIU et al [22] studied the dynamic interactions between precipitates and dislocations in a Cu−0.55Cr−0.05Zr alloy during deformation. It was observed by the authors that the dislocations were pinned by Cr-rich second phase particles, and when they overcame the barrier imposed by precipitates and continued to slide, they were pinned again by other Cr particles, in an intermittent sliding process. This phenomenon could hamper the formation of dislocation arrangements. As the microstructural evolution during ECAP can be defined in terms of dynamic recrystallization [15,19,24], in which the arrangement and accumulation of dislocations in structure of cells are fundamental for the grain refinement, the large amount of nanometric Cr-rich second phase particles precipitated in the Cu matrix act as barriers and make this process difficult. However, the dislocations generated during ECAP processing can shear the Cr precipitates [22] and redistribute them on the Cu matrix.

3.3 Phases evolution

Figure 9 shows the X-ray diffraction patterns of the alloy in the as-received condition and after the ECAP processing. In all samples, the structure is shown mainly by the FCC-Cu phase (matrix) and some discrete diffraction peaks attributed to the BCC-Cr phase (coarse particles). The relative intensity of the diffraction peaks decreases after the deformation by ECAP processing, due to the reduction of coherent domain size and the increase in microstrain.

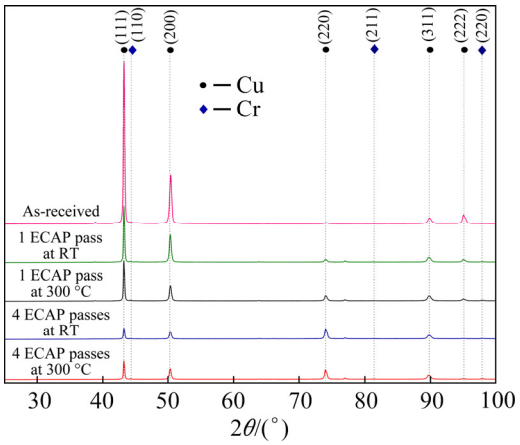

Fig. 9 XRD patterns of Cu−0.81Cr−0.07Zr in as-received condition and after ECAP processing at room temperature and 300 °C

Comparing the diffraction patterns of the samples subjected to ECAP process, it was observed that the relative intensities of the Cu(111) peaks are abruptly decreased while the relative intensities of the Cu(220) peaks tend to increase. After 4 ECAP passes at room temperature, the relative intensities of both peaks are very close each other, although the Cu(111) peak intensity remains the most intense. During the ECAP processing, several slip planes are activated in the microstructure under shear stresses, which may develop a preferential orientation [25,26], besides, changes in crystallographic texture can also be induced by dynamic recrystallization process [27].

Figure 10 shows in detail the region of the diffractogram between the Cu(111) and Cr(110) diffraction peaks. The relative intensity of the Cr(110) peak decreases with the increase of deformation, agreeing with GUO et al [28]. Consequently, the identification of Cr precipitates using XRD analysis becomes complex, as also evidenced by SHEIBANI et al [29], since the

amount of Cr-rich second phase particles decreases with the increasing deformation (see Table 2 and Fig. 8).

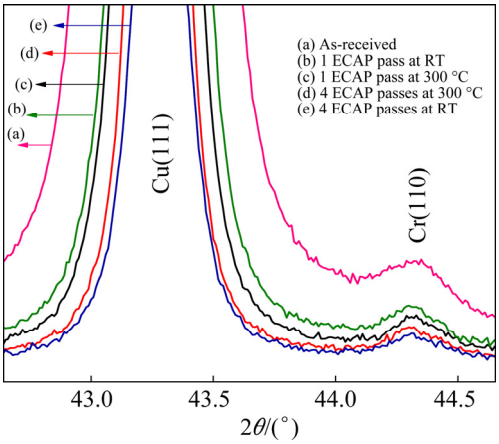

Fig. 10 Cu(111) and Cr(110) diffraction peaks of Cu−0.81Cr−0.07Zr alloy in as-received condition and after ECAP processing at room temperature and 300 °C

Complementing the diffraction patterns shown in Fig. 10, Fig. 11 and Table 3 show, respectively, the diffraction patterns and the structural parameters obtained after Rietveld refining method. The atomic radius of Cr (1.249 Å) is significantly smaller than that of Cu (1.278 Å) [30], which causes a great distortion of the crystalline lattice when in solution in the copper matrix. Consequently, large stress fields arise in the vicinity of the solute atoms. This is one of the reasons for the low solid solubility of chromium in copper. Based on the reduction of the matrix lattice parameter as a function of the number ECAP passes in Table 3, it can be supposed that the deformation leads to the dissolution of Cr in the Cu matrix.

In order to support the hypothesis that the reduction in the lattice parameter of the Cu matrix is associated with the increase of Cr in solid solution, the lattice parameter of the alloy after solution heat treatment at 1020 °C for 1 h is also shown in Table 3. As in this condition, the effect of deformation can be disregarded, since the dislocation density is considerably lower compared to the samples subjected to ECAP, the solute atoms are the main factor affecting the lattice parameter. After the heat treatment, most of the Cr is in solid solution and the matrix lattice parameter is the smallest among all conditions. Besides, in Fig. 10 it is possible to observe the significant reduction of the relative intensity of the Cr(110) peak after 4

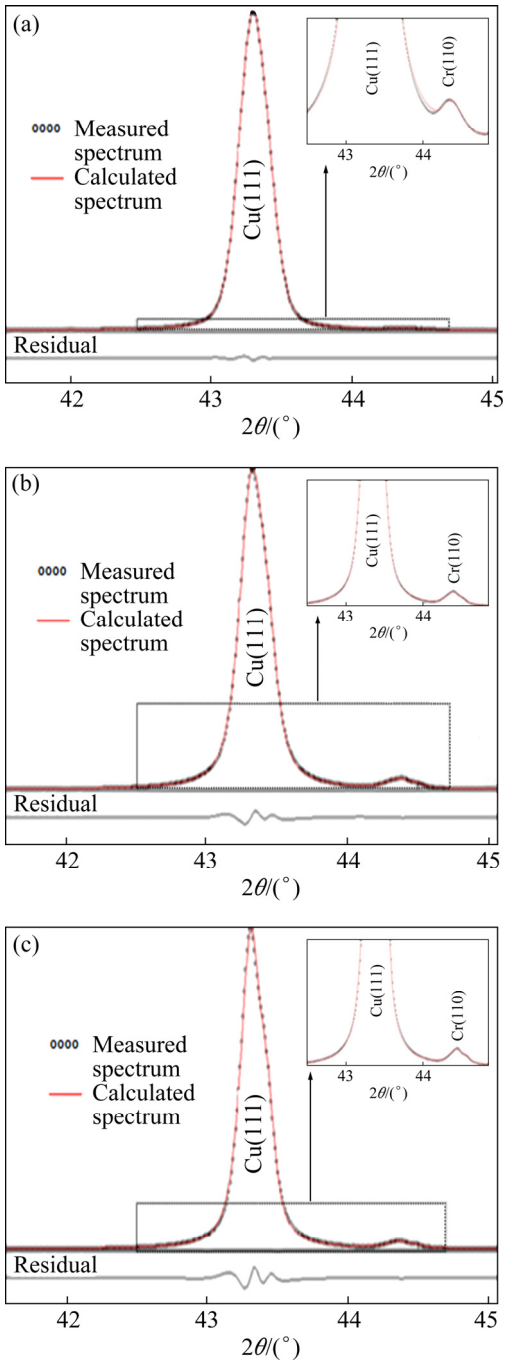

Fig. 11 X-ray diffractograms of samples after refinement by Rietveld method showing details of Cu(111) and Cr(110) diffraction peaks of samples in different conditions: (a) As-received; (b) 4 ECAP passes at room temperature; (c) 4 ECAP passes at 300 °C

ECAP passes in both processing temperatures, which reinforces the hypothesis of the dissolution induced by deformation. These results agree with the results presented by KORNEVA et al [31], but disagree with the results obtained by GUO et al [28] and BACHMAIER et al [30], who reported the

Table 3 Structural parameters of Cu−0.81Cr−0.07Zr alloy in several conditions, obtained after refinement of X-ray diffraction patterns by Rietveld method

Condition	Lattice parameter/Å		
	Cr(110)	Cu(111)	Cu(220)
As-received	2.8838	3.6156	3.6225
1 ECAP pass at RT	2.8836	3.6120	3.6168
4 ECAP passes at RT	2.8821	3.6103	3.6111
1 ECAP pass at 300 °C	2.8829	3.6135	3.6159
4 ECAP passes at 300 °C	2.8838	3.6133	3.6196
Solution treated at 1020 °C for 1 h	2.8833	3.5959	3.6019

increase of the Cu lattice parameter when Cr dissolution is induced by severe plastic deformation. However, in their case, the deformation levels were very high (ε>200, in comparison to ε=2.8 in the present work), leading to the formation of a nanostructure with a high area fraction of disordered grain boundaries. BACHMAIER et al [30] concluded that the excess of vacancies in grain boundaries can lead to the increase in the matrix volume, as it induces larger interatomic spacing and lattice strain.

Figure 12 shows graphically the evolution of the Cu matrix lattice parameter with the number of ECAP passes, evidencing that its reduction starts at the first ECAP pass for both processing temperatures. As the deformation level further increases, the lattice parameter obtained from the Cu(111) peak analysis decreases, being more evident when ECAP is performed at room temperature. The Cu matrix lattice parameter obtained from the analysis of the Cu(220) diffraction peak shows the same trend after the first ECAP pass. After the fourth pass of ECAP at 300 °C, the matrix lattice parameter starts to grow again. This is an indication that the deformation-induced dissolution of Cr particles is more pronounced when the ECAP process is performed at room temperature. It is supposed that the partial dissolution of chromium atoms competes with the decomposition of the supersaturated solid solution when the processing temperature is increased. The high shear stress occurring during severe plastic deformation favors the dissolution of Cr atoms in the Cu matrix, agreeing with BACHMAIER et al [30], whereas the thermal energy associated with the excess of structural defects favors the dynamic precipitation of the second phase particles [32]. Consequently, dissolved Cr atoms are removed from the supersaturated matrix, thus increasing its lattice parameter.

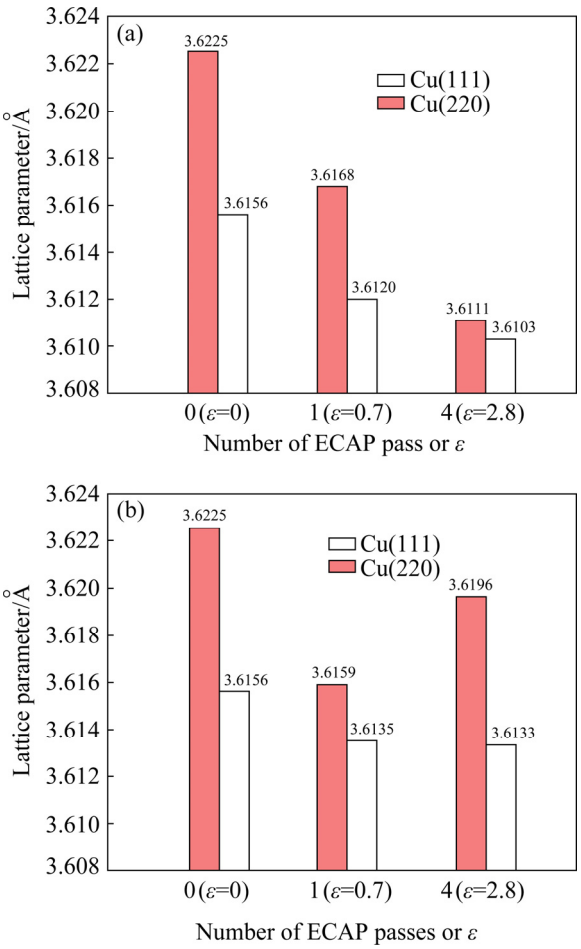

Fig. 12 Evolution of Cu matrix lattice parameters as function of number of ECAP passes calculated from Cu(111) and Cu(220) diffraction peaks: (a) ECAP at room temperature; (b) ECAP at 300 °C

The amount of solute in the Cu matrix can also be assessed indirectly through electrical conductivity measurements, since the electron movement is severely affected by distortions in the crystalline lattice caused by the differences between atomic radii of Cu and Cr. The electrical conductivity is much less affected by structural defects induced by SPD processing, as evidenced by MOROZOVA and KAIBYSHEV [19]. PURCEK et al [33] proposed that the reduction in the electrical conductivity during SPD processing can be associated with deformation-induced dissolution of second phase particles. Table 4 shows the results of the electrical conductivity measurements

performed on the samples, in the as-received condition and after deformation by ECAP processing at both temperatures. The electrical conductivity continuously decreases with the number of ECAP passes at room temperature. ECAP at 300 °C, on the other hand, decreases the electrical conductivity after the first pass, remaining unchanged after the three subsequent passes. As already mentioned in the discussion of the matrix lattice parameter evolution, both Cr dissolution and re-precipitation compete each other during SPD at elevated temperature. Thus, it is supposed that, after the first pass at 300 °C, the flux of Cr atoms entering or leaving the Cu matrix reaches a steady state.

Table 4 Electrical conductivity of Cu−0.81Cr−0.07Zr alloy in as-received condition and after ECAP processing

Condition	Electrical conductivity/%(IACS)
As-received	83.6±0.2
1 ECAP pass at RT	76.2±0.7
4 ECAP passes at RT	71.7±1.3
1 ECAP pass at 300 °C	77.2±0.8
4 ECAP passes at 300 °C	77.9±0.7

As far as the hardness is concerned, the effect of ECAP temperature is also very important. The grain refinement is more effective when the plastic deformation is performed at room temperature, resulting in higher mechanical strength as observed from the average grain size and hardness values shown in Table 1. ECAP performed at 300 °C enables the occurrence of recovery and recrystallization processes, as these mechanisms are thermally activated. As a result, there is a reduction in the dislocation density, decreasing the strengthening effect.

In order to further investigate the behavior of Cr precipitates during ECAP at different temperatures, DSC analysis was performed, and the results are shown in Fig. 13. As no peak of exothermic reaction is observed in the as-received sample during heating at a constant rate, it is assumed that, under such conditions, the alloy is near to the thermodynamic equilibrium, with all excessive Cr in the form of second phase particles. Differently, the samples subjected to ECAP show a very well-defined exothermic peak between 360 and 380 °C, regardless of the processing temperature. The exothermic peak in this temperature range is related to the precipitation of second phase particles in the copper matrix of the Cu−Cr−Zr alloy [7]. Thus, the enthalpy release from exothermic reactions observed only in the samples subjected to ECAP processing, associated to the decrease of the Cu lattice parameter and to the reduction of electrical conductivity, supports the hypothesis that, during ECAP processing, a partial dissolution of chromium particles, induced by the severe deformation, occurs beyond the mechanical fragmentation.

In Fig. 13, it is also possible to see that the decomposition temperature of the supersaturated solid solution occurs at lower temperatures than the typical aging temperature of these alloys (near to 450 °C) [3,9,34,35]. This fact may be associated with the history of plastic deformation of the material. The materials processed by SPD have their precipitation kinetics accelerated, when compared to the same materials conventionally processed, as

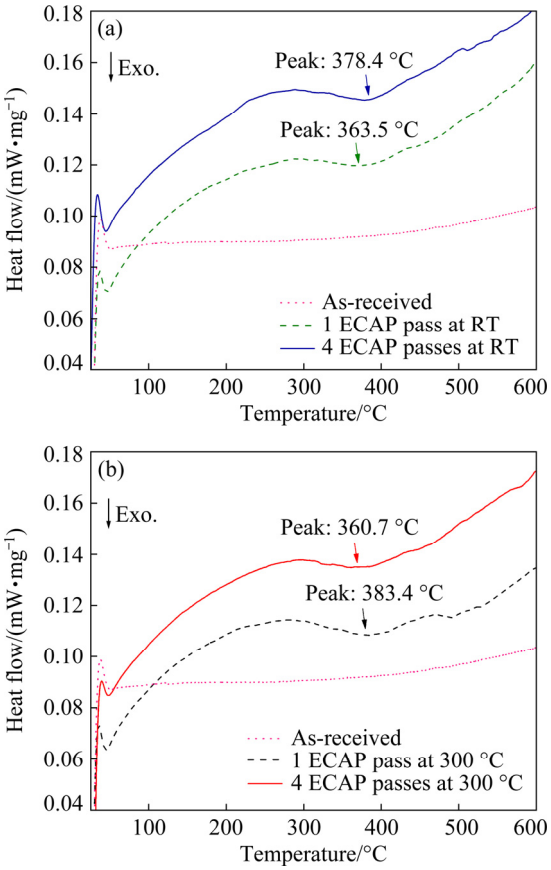

Fig. 13 Thermal analysis of Cu−0.81Cr−0.07Zr during constant heating at 10 °C/min in as-received condition and after ECAP processing: (a) At room temperature; (b) At 300 °C

reported by PURCEK et al [6] and LEÓN et al [9]. AKSENOV et al [10] reported that a high density of defects generated during SPD act as preferential sites for particles nucleation, contributing to the phase transformation that occurs through diffusion process.

The phase transformation in Cu−Cr−Zr alloys subjected to ECAP processing is rather complex, agreeing with ABIB et al [36]. The formation of an UFG structure is accompanied by a high density of dislocations and non-equilibrium grain boundaries. The interaction of these structural defects with the second phase particles affects the decomposition of supersaturated solid solution. As the Cr particles re-precipitate, they can delay the recovery and recrystallization processes due to the pinning effect, as reported by SHANGINA et al [5]. In the present study, no exothermic reaction is associated to recovery and recrystallization processes. However, according to the Refs. [7,36,37], these processes occur above 500 °C.

Samples processed by ECAP in all processing conditions were submitted to a subsequent aging treatment for 1 h at the temperatures of the exothermic reactions, in order to explore the additional hardening potential observed by thermal analysis, since the decomposition of solid solution during aging results in the precipitation of fine second phase particles in the matrix, increasing the hardness due to their interaction with dislocations movements. Samples submitted to 1 ECAP pass at room temperature and 4 ECAP passes at 300 °C were aged at 360 °C. Samples submitted to 4 ECAP passes at room temperature and 1 ECAP pass at 300 °C were aged at 380 °C. Table 5 brings together the values of electrical conductivity and hardness after these aging treatments. It can be observed that after aging, the electrical conductivity of all samples was totally restored to values above 83% (IACS). Furthermore, the hardness values also increase, surpassing the hardness of the as-received alloy (170 HV in the initial condition). In this case, the alloy aged after 4 passes of ECAP stands out, whose hardness increased from the initial 170 HV to 191 HV. The simultaneous increase in hardness and electrical conductivity values after aging reinforces the hypothesis of partial dissolution of the Cr particles, induced by deformation during ECAP. The subsequent aging results in the re-precipitation of particles, reducing the matrix distortion and restoring the electrical conductivity. Furthermore, the re-precipitated particles stabilize the microstructure formed during ECAP, promoting an additional hardening effect. The overall result is the increase of strength of the as-received material, maintaining the same level of electrical conductivity.

4 Conclusions

(1) After 4 ECAP passes both at room temperature and 300 °C, the area fraction of coarse Cr-rich particles in microstructure presented a significant decrease.

(2) Grain refinement was also obtained after ECAP, particularly on samples processed at room temperature, increasing the hardness from initial 170 HV to 188 HV.

(3) The ECAP processing leads to the reduction of the electrical conductivity, from the initial 83.6%(IACS) to 71.7%(IACS) after 4 ECAP passes at room temperature. This reduction was associated with the partial deformation-induced dissolution of second phase particles in Cu lattice.

(4) The partial dissolution of Cr-rich precipitates in Cu lattice induced by the deformation

Table 5 Hardness and electrical conductivity of Cu−0.81Cr−0.07Zr after ECAP processing and aging at 360 and 380 °C for 1 h

Condition	Aging temperature/ °C	After ECAP processing		After ECAP processing and aging	
		Electrical conductivity/ %(IACS)	Hardness (HV)	Electrical conductivity/ %(IACS)	Hardness (HV)
1 ECAP pass at RT	360	76.2±0.7	178±3	83.1±0.1	179±4
4 ECAP passes at RT	380	71.7±1.3	188±4	83.5±0.2	191±3
1 ECAP pass at 300 °C	380	77.2±0.8	169±5	83.9±0.1	175±3
4 ECAP passes at 300 °C	360	77.9±0.7	176±4	83.3±0.1	179±4

by ECAP was supported by the decrease in the Cu matrix lattice parameter, by the exothermic reactions observed during subsequent heating and by the decrease in the electrical conductivity.

(5) There is evidence that during the deformation by ECAP at 300 °C, dissolution and re-precipitation of second phase particles occur simultaneously, since the electrical conductivity remains practically constant, between 77.2%(IACS) and 77.9%(IACS), with a slight increase in hardness with the increase of deformation.

(6) During subsequent aging, samples subjected to ECAP exhibited an additional hardening effect caused by the re-precipitation of the partially dissolved particles, keeping the grain refinement obtained by severe plastic deformation. The better combination of hardness (191 HV) and electrical conductivity (83.5%(IACS)) was obtained in the sample aged after 4 ECAP passes at room temperature.

Acknowledgments

The authors would like to give special thanks to Professor PhD André da Silva Antunes from the Mechanical Engineering Department of the Aeronautic Technology Institute (IEM-ITA), to Professor PhD Ângelo Fernando Padilha from the Metallurgical and Materials Engineering Department of the Polytechnic School of the University of São Paulo (PMT-POLI-USP) and to Mr. Leonardo Zappi from Zappi Technology by support with the hardness and electrical conductivity measurements in this work; besides they were always willing to help and motivated the scientific development. The authors would also like to thank the NAPCEM Multi-User Laboratory (ICT/ UNIFESP) Brazil for the facilities.

References

[1] PURCEK G, YANAR H, SARAY O, KARAMAN I, MAIER H J. Effect of precipitation on mechanical and wear properties of ultrafine-grained Cu−Cr−Zr alloy [J]. Wear, 2014, 311(1/2): 149−158.

[2] CHEN J S, WANG J F, XIAO X P, WANG H, CHEN H M, YANG B. Contribution of Zr to strength and grain refinement in CuCrZr alloy [J]. Materials Science and Engineering A, 2019, 756: 464−473.

[3] MENG A, NIE J F, WEI K, KANG H J, LIU Z J, ZHAO Y H. Optimization of strength, ductility and electrical conductivity of a Cu−Cr−Zr alloy by cold rolling and aging treatment [J]. Vacuum, 2019, 167: 329−335.

[4] WEI K X, WEI W, WANG F, DU Q B, ALEXANDROV I V, HU J. Microstructure, mechanical properties and electrical conductivity of industrial Cu−0.5%Cr alloy processed by severe plastic deformation [J]. Materials Science and Engineering A, 2011, 528: 1478−1484.

[5] SHANGINA D V, BOCHVAR N R, MOROZOVA A I, BELYAKOV A N, KAIBYSHEV R O, DOBATKIN S V. Effect of chromium and zirconium content on structure, strength and electrical conductivity of Cu−Cr−Zr alloys after high pressure torsion [J]. Materials Letters, 2017, 199: 46−49.

[6] PURCEK G, YANAR H, DEMIRTAS M, ALEMDAG Y, SHANGINA D V, DOBATKIN S V. Optimization of strength, ductility and electrical conductivity of Cu−Cr−Zr alloy by combining multi-route ECAP and aging [J]. Materials Science and Engineering A, 2016, 649: 114−122.

[7] VINOGRADOV A, PATLAN V, SUZUKI Y, KITAGAWA K, KOPYLOV V I. Structure and properties of ultra-fine grain Cu−Cr−Zr alloy produced by equal-channel angular pressing [J]. Acta Materialia, 2002, 50(7): 1639−1651.

[8] VALIEV R Z, LANGDON T G. Principles of equal-channel angular pressing as a processing tool for grain refinement [J]. Progress in Materials Science, 2006, 51(7): 881−981.

[9] LEÓN K V, MUÑOZ-MORRIS M A, MORRIS D G. Optimisation of strength and ductility of Cu−Cr−Zr by combining severe plastic deformation and precipitation [J]. Materials Science and Engineering A, 2012, 536: 181−189.

[10] AKSENOV D A, ASFANDIYAROV R, RAAB G I, ISYANDAVLETOVA G B. Features of the physico-mechanical behavior of UFG low-alloyed bronze Cu−1Cr−0.08Zr produced by severe plastic deformation [J]. IOP Conference Series: Materials Science and Engineering, 2017, 179(1): 012001.

[11] FAIZOVA S N, RAAB G I, FAIZOV I A, AKSENOV D A, ZARIPOV N G, FAIZOV R A, SEMENOV V I, ZEMLYAKOVA N V. The effect of the second phase particle size on fracture behavior of Cu−0.1%Sn ultra-fine-grained alloy [J]. Russian Physics Journal, 2016, 59(1): 116−120.

[12] FAIZOV I A, RAAB G I, FAIZOVA S N, ZARIPOV N G, AKSENOV D A. The role of phase transitions in the evolution of dispersion particles in chromium bronzes up the equal channel angular pressing [J]. Letters on Materials, 2016, 6(2): 132−137.

[13] MISHNEV R, SHAKOVA I, BELYAKOV A, KAIBYSHEV R. Deformation microstructures, strengthening mechanisms, and electrical conductivity in a Cu−Cr−Zr alloy [J]. Materials Science and Engineering A, 2015, 629: 29−40.

[14] IWAHASHI Y, HORITA Z, NEMOTO M, WANG J, LANGDON T G. Principle of equal-channel angular pressing for the processing of ultra-fine grained materials [J]. Scripta Materialia, 1996, 35(2): 143−146.

[15] MOROZOVA A, BORODIN E, BRATOV V, ZHEREBTSOV S, BELYAKOV A, KAIBYSHEV R. Grain refinement kinetics in a low alloyed Cu−Cr−Zr alloy

subjected to large strain deformation [J]. Materials, 2017, 10(12): 1394.

[16] SUN P L, KAO P W, CHANG C P. High angle boundary formation by grain subdivision in equal channel angular extrusion [J]. Scripta Materialia, 2004, 51(6): 565−570.

[17] YAMAGUCHI D, HORITA Z, NEMOTO M, LANGDON T G. Significance of adiabatic heating in equal-channel angular pressing [J]. Scripta Materialia, 1999, 41(8): 791−796.

[18] PEI Q X, HU B H, LU C, WANG Y Y. A finite element study of the temperature rise during equal channel angular pressing [J]. Scripta Materialia, 2003, 49(4): 303−308.

[19] MOROZOVA A, KAIBYSHEV R. Grain refinement and strengthening of a Cu−0.1Cr−0.06Zr alloy subjected to equal channel angular pressing [J]. Philosophical Magazine, 2017, 97(24): 2053−2076.

[20] LIU C Y, YU L, MA M Z, LIU R P, MA Z Y. Dynamic precipitation of Al−Zn alloy during rolling and accumulative roll bonding [J]. Philosophical Magazine Letters, 2015, 95(11): 539−546.

[21] FAIZOVA S N, FAIZOV I A, SEMENOV V I, HIZBULLIN F F. Influence of structural and phase transformation on properties of severely deformed dispersion-hardening alloys [J]. Materials Science: Non-Equilibrium Phase Transformations, 2017, 3(5): 180−183.

[22] LIU J B, HOU M L, YANG H Y, XIE H B, YANG C, ZHANG J D, FENG Q, WANG L T, MENG L, WANG H T. In-situ TEM study of the dynamic interactions between dislocations and precipitates in a Cu−Cr−Zr alloy [J]. Journal of Alloys and Compounds, 2018, 765: 560−568.

[23] ABIB K, AZZEDDINE H, TIRSATINE K, BAUDIN T, HELBERT A L, BRISSET F, ALILI B, BRADAI D. Thermal stability of Cu−Cr−Zr alloy processed by equal-channel angular pressing [J]. Materials Characterization, 2016, 118: 527−534.

[24] SHAKHOVA I, YANUSHKEVICH Z, FEDOROVA I, BELYAKOV A, KAIBYSHEV R. Grain refinement in a Cu−Cr−Zr alloy during multidirectional forging [J]. Materials Science and Engineering A, 2014, 606: 380−389.

[25] KHEREDDINE A Y, LARBI F H, AZZEDDINE H, BAUDIN T, BRISSET F, HELBERT A L, MATHON M H, KAWASAKI M, BRADAI D, LANGDON T G. Microstructures and textures of a Cu−Ni−Si alloy processed by high-pressure torsion [J]. Journal of Alloys and Compounds, 2013, 574: 361−367.

[26] LI S, BEYERLEIN I J, BOURKE M A M. Texture formation during equal channel angular extrusion of fcc and bcc materials: Comparison with simple shear [J]. Materials Science and Engineering A, 2005, 394: 66−77.

[27] HIGUERA-COBOS O F, BERRÍOS-ORTIZ J A, CABRERA J M. Texture and fatigue behavior of ultrafine grained copper produced by ECAP [J]. Materials Science and Engineering A, 2014, 609: 273−282.

[28] GUO J, ROSALIE J M, PIPPAN R, ZHANG Z. Revealing the Microstructural evolution in Cu−Cr nanocrystalline alloys during high pressure torsion [J]. Materials Science and Engineering A, 2017, 695: 350−359.

[29] SHEIBANI S, HESHMATI-MANESH S, ATAIE A. Structural investigation on nano-crystalline Cu−Cr supersaturated solid solution prepared by mechanical alloying [J]. Journal of Alloys and Compounds, 2010, 495: 59−62.

[30] BACHMAIER A, RATHMAYR G B, BARTOSIK M, APEL D, ZHANG Z, PIPPAN R. New insights on the formation of supersaturated solid solutions in the Cu−Cr system deformed by high-pressure torsion [J]. Acta Materialia, 2014, 69: 301−313.

[31] KORNEVA A, STRAUMAL B, KILMAMETOV A, CHULIST R, STRAUMAL P, ZIEBA P. Phase transformations in a Cu−Cr alloy induced by high pressure torsion [J]. Materials Characterization, 2016, 114: 151−156.

[32] AZZEDDINE H, MEHDI B, HENNET L, THIAUDIÈRE D, ALILI B, KAWASAKI M, BRADAI D, LANGDON T G. An in situ synchrotron X-ray diffraction study of precipitation kinetics in a severely deformed Cu−Ni−Si alloy [J]. Materials Science and Engineering A, 2014, 597: 288−294.

[33] PURCEK G, YANAR H, SHANGINA D V, DEMIRTAS M, BOCHVAR N R, DOBATKIN S V. Influence of high pressure torsion-induced grain refinement and subsequent aging on tribological properties of Cu−Cr−Zr alloy [J]. Journal of Alloys and Compounds, 2018, 742: 325−333.

[34] ZHOU K, CHEN W G, FENG P, YAN F L, FU Y Q. Arc ablation behavior and microstructure evolution of plastically deformed and micro-alloyed Cu−Cr−Zr alloys [J]. Journal of Alloys and Compounds, 2020, 820: 153123.

[35] FU H D, XU S, LI W, XIE J X, ZHAO H X, PAN Z J. Effect of rolling and aging processes on microstructure and properties of Cu−Cr−Zr alloy [J]. Materials Science and Engineering A, 2017, 700: 107−115.

[36] ABIB K, LARBI F H, RABAHI L, ALILI B, BRADAI D. DSC analysis of commercial Cu−Cr−Zr alloy processed by equal channel angular pressing [J]. Transactions of Nonferrous Metals Society of China, 2015, 25(3): 838−843.

[37] KVAČKAJ T, KOVÁČOVÁ A, KOČIŠKO R. Post SPD material's recovery in thermal exposition [J]. Acta Physica Polonica A, 2015, 128(4): 689−692.

等径角挤压对 Cu−0.81Cr−0.07Zr 合金第二相颗粒分布、硬度和电导率的影响

Filipe CALDATTO DALAN[1], Gisele Ferreira de LIMA ANDREANI[1], Dilermando Nagle TRAVESSA[1], Ilshat Albertovich FAIZOV[2], Svetlana FAIZOVA[3], Kátia Regina CARDOSO[1]

1. Institute of Science and Technology, Federal University of São Paulo, 330 Talim St., São José dos Campos, 12231-280, Brazil;
2. Institute for Metals Superplasticity Problems RAS, 39 S. Khalturin St., Ufa, 450001, Russia;
3. Ufa State Aviation Technical University, 12 K. Marx St., Ufa, 450008, Russia

摘　要：研究在室温和 300 °C 下等径角挤压(ECAP)对 Cu−0.81Cr−0.07Zr 合金中第二相分布的影响，及其对硬度和电导率的影响。显微组织表征表明，经 ECAP 后，粗大的富 Cr 颗粒面积分数减小，这是由于塑性变形导致 Cr 的溶解。在室温下进行 4 道次 ECAP 后，由于固溶体中较高的 Cr 含量和基体中较高的缺陷密度导致电子散射的增加，合金的电导率下降了 12%。仅在 ECAP 样品中观察到的 Cu 晶格常数的减小和差示扫描量热分析(DSC)过程中发生的放热反应证实了这些结果。经 ECAP 后的时效热处理促进额外的硬化效果和导电性的完全恢复，这是由于部分溶解颗粒的再沉淀造成的。在室温下进行 4 道次 ECAP，然后在 380 °C 时效处理 1 h 的合金具有更高的硬度(191 HV)和电导率(83.5%(IACS))。

关键词：等径角挤压；Cu−Cr−Zr 合金；第二相颗粒；相变

(Edited by Wei-ping CHEN)